

# High Prevalence of *PRPH2* in Autosomal Dominant Retinitis Pigmentosa in France and Characterization of Biochemical and Clinical Features

Gael Manes, Tremeur Guillaumie, Werner L. Vos, Aurore Devos, Isabelle Audo, Christina Zeitz, Virginie Marquette, Xavier Zanlonghi, Sabine Defoort-Dhellemmes, Bernard Puech, Saddek Mohand Said, José Alain Sahel, Sylvie Odent, Hélène Dollfus, Josseline Kaplan, Jean-Louis Dufier, Guyleyne Le Meur, Michel Weber, Laurence Faivre, Francine Behar Cohen, Christophe Bérard, Marie-Christine Picot, Coralie Verdier, Audrey Senechal, Corinne Baudoin, Beatrice Bocquet, John B. Findlay, Isabelle Meunier, Claire-Marie Dhaenens, And Christian P. Hamel

- **PURPOSE:** To assess the prevalence of *PRPH2* in autosomal dominant retinitis pigmentosa (adRP), to report 6 novel mutations, to characterize the biochemical features of a recurrent novel mutation, and to study the clinical features of adRP patients.
- **DESIGN:** Retrospective clinical and molecular genetic study.
- **METHODS:** Clinical investigations included visual field testing, fundus examination, high-resolution spectral-domain optical coherence tomography (OCT), fundus autofluorescence imaging, and electroretinogram (ERG) recording. *PRPH2* was screened by Sanger sequencing in a cohort of 310 French families with adRP. Peripherin-2 protein was produced in yeast and analyzed by Western blot.

**RESULTS:** We identified 15 mutations, including 6 novel and 9 previously reported changes in 32 families, accounting for a prevalence of 10.3% in this adRP population. We showed that a new recurrent p.Leu254Gln mutation leads to protein aggregation, suggesting abnormal folding. The clinical severity of the disease in examined patients was moderate with 78% of the eyes having 1-0.5 of visual acuity and 52% of the eyes retaining more than 50% of the visual field. Some patients characteristically showed vitelliform deposits or macular involvement. In some families, pericentral RP or macular dystrophy were found in family members while widespread RP was present in other members of the same families.

- **CONCLUSIONS:** The mutations in *PRPH2* account for 10.3% of adRP in the French population, which is higher than previously reported (0%-8%) This makes *PRPH2* the second most frequent adRP gene after *RHO* in our series. *PRPH2* mutations cause highly variable phenotypes and moderate forms of adRP, including mild cases, which could be underdiagnosed.

## INTRODUCTION

In the retina, the human peripherin-2 gene (prph2; mim #179605), also known as RDS (retinal degeneration slow), encodes peripherin-2, a transmembrane glycoprotein localized in the rim regions of photoreceptor outer segment discs.<sup>1–3</sup> Peripherin-2 forms homo- and heterotetramers with its paralog protein ROM1 (retinal outer segment membrane protein 1; MIM #180721). These oligomers are essential for the stabilization of the disc rims and are required to pile up the discs as compact, elongated structures.<sup>4–8</sup> Mutations in PRPH2 cause a wide range of autosomal dominant retinal dystrophies, either with involvement of the peripheral retina such as retinitis pigmentosa,<sup>9</sup> cone-rod dystrophy,<sup>10,11</sup> and even 1 case of retinitis punctata albescens,<sup>12</sup> or with predominant involvement of the macula such as adult vitelliform macular dystrophy,<sup>13</sup> cone dystrophy,<sup>14</sup> pattern dystrophy,<sup>15,16</sup> and central areolar choroidal atrophy.<sup>17–20</sup> In addition, the PRPH2 p.Leu185Pro substitution has also been associated with ROM1 mutations in a digenic form of retinitis pigmentosa.<sup>21,22</sup>

Among the variety of retinal degenerations caused by PRPH2 mutations, autosomal dominant retinitis pigmentosa (adRP) is the most frequent condition. Typical symptoms of RP include night blindness and progressive visual field constriction, eventually progressing toward total blindness after several decades.<sup>23</sup> The prevalence of RP is approximately 1/3500 to 1/4000 and the mode of inheritance can be autosomal dominant (30%–40%), autosomal recessive (50%–60%), or X-linked (5%–15%).<sup>23,24</sup> RP is the most genetically heterogeneous clinical entity of inherited retinal disorders, with 69 disease-causing genes currently known in this condition ([www.sph.uth.tmc.edu/retnet](http://www.sph.uth.tmc.edu/retnet)), including 24 genes causing adRP. The prevalence of the known genes in adRP ranges from 26.5%<sup>25,26</sup> to 16.6%<sup>27</sup> for the most frequently found mutations in RHO (MIM #180380), to many genes accounting for less than 1% of the adRP families. Among those genes, the prevalence of PRPH2 mutations varies widely from 0% to 8% of the cases of adRP in cohorts of different origins, but no accurate prevalence data are available for the French population.<sup>28–30</sup> Also, as usually found in adRP, the severity of the PRPH2 genetic form is considered as moderate, but it is not known whether there are important variations of severity inside the PRPH2 genetic category. Therefore, we sought PRPH2 mutations in a large cohort of 310 adRP families originating mainly from France. We found novel mutations, characterized the biochemical features of 1 novel mutation, and analyzed the clinical features of the affected patients.

**CLINICAL INVESTIGATIONS:** Patients had standard ophthalmologic examination (refractometry, visual acuity, slit-lamp examination, applanation tonometry, and funduscopy). Kinetic visual fields were determined with a Goldmann perimeter with targets V4e, III4e, and I4e. Optical coherence tomography (OCT) measurement of the macula was performed using an OCT-3 system (Stratus model 3000; Carl Zeiss Meditec, Dublin, California, USA) or with a spectral-domain OCT (Spectralis, Heidelberg, Germany) with software version 3.0. Autofluorescence measurements were obtained with the HRA2 Heidelberg retinal confocal angiograph (Heidelberg Engineering, Dossenheim, Germany) and fundus pictures were taken. Full-field electroretinograms (ERGs) were recorded using a Ganzfeld apparatus (Metrovision, Pénchies, France) with a bipolar contact lens electrode on maximally dilated pupils according to the ISCEV protocol.<sup>31</sup>

For numerical values, visual acuity was measured with Snellen charts in decimal numbers. Goldmann visual field

was quantified by counting the number of subdivisions of the Goldmann grid within the areas of the V4e isopter and expressed as a percentage of the normal visual field. Correlations between visual parameters (visual acuity, visual field, and ERG amplitudes) and age were investigated with the coefficient correlation of ranks of Spearman with a confidence interval at 95%, calculated by a Fisher transformation.

**MUTATION SCREENING:** Genomic DNA was isolated from 10 mL peripheral blood leukocytes using standard salting-out procedure.<sup>32</sup> Coding exons and adjacent intronic sequences of the PRPH2 gene (NM\_000322.4; primer pairs and polymerase chain reaction [PCR] conditions are available on request) were sequenced with an Applied Biosystems 3130xL genetic analyzer (Applied Biosystems, Foster City, California, USA) using a BigDye Terminator cycle sequencing ready reaction kit V3.1 (Applied Biosystems) following the manufacturer's instructions. Sequence analysis and mutation identification were performed using Collection and Sequence Analysis software package (Applied Biosystems). SIFT, PolyPhen2, and Align GVGD were used to predict possible impacts of missense variants. The genomic sequence environment

## METHODS

**PATIENTS:** Three hundred and ten index patients were included in the study. Informed and written consent was obtained for all patients participating in the study. Patients of European origins were recruited from 10 different clinical centers in France. The study (# 2008-A01238-47) received the authorization from the Sud méditerranéenne IV ethical board committee (# 08 10 05 from 04/11/2008), was approved by the French regulation agency for medication (AFSSAPS # B81319-70), and is registered at <http://clinicaltrials.gov> (# NCT01235624). The investigators followed the tenets of the Declaration of Helsinki. of putative splice-site mutations was analyzed using Human Splicing Finder and MaxEnt.

**GENOTYPING OF MICROSATELLITE MARKERS AND LINKAGE ANALYSIS:** PCR was carried out in 25 mL final volume containing 50 ng genomic DNA, 5 pmol of each primer, 0.2 mM dNTPs (MP Biochemicals, Asse-Relegem, Belgium), 2 mM MgCl<sub>2</sub>, PCR buffer, and 1 unit of DNA polymerase (AmpliTaq Gold; Applied Biosystems). Initial denaturation at 95 C for 10 minutes was followed by 35 cycles of denaturation at 94 C for 30 seconds, specific annealing temperature for 30 seconds, and extension at 72 C for 1 minute. A final extension step was performed at 72 C for 10 minutes. The PCR products were diluted and mixed with Genescan 400HD ROX size standard and subsequently analyzed on an Applied Biosystems 3130xL genetic analyzer (Applied Biosystems). Results were analyzed with GeneMapper software (version 4.0; Applied Biosystems).

Two-point LOD scores were calculated with Superlink-online (<http://bioinfo.cs.technion.ac.il/superlink-online/>). The phenotype was analyzed as an autosomal dominant and fully penetrant trait with an affected allele frequency of 0.001.

## PERIPHERIN-2 EXPRESSION AND WESTERN BLOTS:

Wild-type (WT) and p.Leu254Gln (L254Q) mutant were cloned into the pPICZ expression vector containing the c-myc epitope and the polyhistidine (His)<sub>6</sub>-tag as described before<sup>33</sup>; the nucleotide sequence was confirmed by Eurofins MWG (Ebersberg, Germany) using automated DNA sequencing. *Pichia pastoris* cells (strain KM71H) were transformed with the PmeI linearized expression vector, stably transformed cells were spread on YPD plates (1%

yeast extract, 2% peptone, 2% glucose, 2% agar) with media containing 100 mg/mL zeocin. Cells were cultured, harvested, and stored at 80 C as described before.<sup>33</sup> Cells were lysed upon further processing and membranes containing the WT or L254Q proteins were isolated using differential centrifugation as described previously. The membranes were dissolved in 1% n-dodecyl-b-D-maltoside (DDM) using sequentially an 18G, 19G, and 25G needle. His-tagged WT or L254Q proteins were purified using Ni-NTA agarose (final buffer 10 mM NaPO<sub>4</sub>, 150 mM NaCl, 200 mM imidazole, and 0.1% n-dodecyl-b-D-malto-side). Reducing sodium dodecyl sulfate–polyacrylamide gel electrophoresis (SDS-PAGE) was performed by mixing 1:1 (v:v) with 23 loading buffer containing 1% b-mercaptoethanol and incubated for 5 minutes at room temperature prior to loading of the gel. Nonreducing SDS-PAGE was performed by mixing 1:1 (v:v) with 23 loading buffer without b-mercaptoethanol and immediate loading after mixing. Transfer to the polyvinylidene fluoride membrane and probing—using cmyc-tagged murine monoclonal (Cell Signaling Technology, Danvers, Massachusetts, USA) as primary and anti-mouse horseradish peroxidase–conju-gated (Promega, Fitchburg, Wisconsin, USA) as secondary antibody—was done as described before.

## RESULTS

### IDENTIFICATION OF RECURRENT AND NOVEL PRPH2

**MUTATIONS:** A cohort of 310 French families with auto-somal dominant retinitis pigmentosa was screened for the 3 exons of the PRPH2 gene (NM\_000322.4). We found that 32 probands (10.3%) carried a mutation. A total of 15 different mutations were identified (Table 1). Nine of them were previously described, including 1 nonsense (p.Arg46\*) and 8 missense mutations (p.Leu126Pro, p.Cys165Tyr, p.Trp179Arg, p.Ser198Arg, p.Gly208Asp, p.Phe211Leu, p.Pro216Ser, and p.Cys222Ser). Six others were novel, including 4 missense (p.Asp194Glu, p.Trp246Cys, p.Ala253Glu, and p.Leu254Gln), 1 frame-shift (p.Val69Cysfs\*30), and 1 splice site (c.829-4C>G) mutation. All mutations co-segregated with the disease phenotype in available family members (Figures 1 and 2). The novel mutations were not identified in 96 ethnically matched control individuals and were not present in the public human SNP databases (including dbSNP, Ensembl, HapMap, the 1000 Genomes project and Exome Variant Server).

Among the novel mutations, the truncating p.Val69Cysfs\*30 mutation led to a premature termination located within the second transmembrane  $\alpha$ -helix of peripherin-2. No affected family members were available to test the familial segregation for the p.Asp194Glu mutation (Figure 2, Bottom right), but Asp194 is conserved in 16 peripherin-2 orthologs (Figure 3) and is surrounded by residues Lys193 and Arg195, which have been found mutated previously.<sup>20,34</sup> Moreover, the substitution p.Asp194Glu was predicted to be damaging by PolyPhen2 and align-GVGD programs but not by SIFT (Table 1). For the mutations p.Trp246Cys and p.Ala253Glu, both residues at positions 246 and 253 are also evolutionary conserved (p.Trp246Cys, p.Ala253Glu, and p.Leu254Gln), 1 frame-shift (p.Val69Cysfs\*30), and 1 splice site (c.829-4C>G) mutation. All mutations co-segregated with the disease phenotype in available family members (Figures 1 and 2). The novel mutations were not identified in 96 ethnically matched control individuals and were not present in the public human SNP databases (including dbSNP, Ensembl, HapMap, the 1000 Genomes project and Exome Variant Server). Among the novel mutations, the truncating p.Val69Cysfs\*30 mutation led to a premature termination located within the second transmembrane  $\alpha$ -helix of peripherin-2. No affected family members were available to test the familial segregation for the p.Asp194Glu mutation (Figure 2, Bottom right), but Asp194 is conserved in 16 peripherin-2 orthologs (Figure 3) and is surrounded by residues Lys193 and Arg195, which have been found mutated previously.<sup>20,34</sup> Moreover, the substitution p.Asp194Glu was predicted to be damaging by PolyPhen2 and align-GVGD programs but not by SIFT (Table 1). For the mutations p.Trp246Cys

and p.Ala253Glu, both residues at positions 246 and 253 are also evolutionary conserved (Figure 3), and Trp246 has been previously found mutated in p.Trp246Arg.<sup>35</sup> These 2 mutations were predicted to be damaging by PolyPhen2, align-GVGD, and SIFT but tolerated by SIFT for p.Ala253Glu (Table 1).

We identified 4 families (PHRC057, PHRC069, PHRC161, and PHRC162) with the novel missense mutation, c.761T>A (p.Leu254Gln), with all affected subjects heterozygous for the mutation except 2 homozygous brothers (II:2 and II:3) in Family PHRC161. These 2 subjects had presumed consanguineous parents, while unaffected individuals did not carry the mutation (Figure 2, Left). The evolutionary conserved Leu254 is located in the D2 loop (Figures 3 and 8) and the substitution p.Leu254Gln is predicted to be damaging by PolyPhen2, SIFT, and align-GVGD programs (Table 1). In order to investigate whether p.Leu254Gln was a founder mutation, we genotyped the microsatellite markers D6S1575, D6S1549, D6S1552, D6S282, and D6S1650 that spanned the 2.98 Mb surrounding PRPH2 in the available DNA samples in the 4 families. We found that all affected members of the 4 families shared an identical allele for the 5 markers, except Patient II:2 of Family PHRC161, who had a cross-over between D6S1552 and D6S1549 (Figure 2, Left). Since the 4 families originated from the same area in the south of France, this indicates a founder effect. We confirmed the linkage at this locus with microsatellite markers reaching a maximum cumulated LOD (logarithm of odds) score of 4.484 for D6S1575 (Figure 2, Left). Since many patients carried the p.Leu254Gln, we performed biochemical investigations of the mutated peripherin-2. The WT and the mutated L254Q peripherin-2 proteins were expressed in yeast. We found that both purified WT and L254Q mutant showed monomers and formed dimers (Figure 4). However, aggregates, which were present in both WT and mutated protein extracts, were much more abundant with the L254Q mutant. In addition, in the absence of the reducing agent  $\beta$ -mercaptoethanol in the sample buffer, the amounts of monomeric and dimeric L254Q were dramatically decreased compared to the WT. Thus, the L254Q mutant exhibited a strong tendency to form large aggregates, which might suggest abnormal folding for L254Q mutant.

Five independent families (PHRC011, PHRC084, PHRC197, PHRC276, and Fam716) had the c.829-4C>G mutation (Figure 2, Top right). Two algorithms (Human Splicing Finder and MaxEnt) predicted that the c.829-4C>G mutation would create an acceptor splice site located 3 base pairs upstream of the natural splice site and lead to the in-frame insertion of 1 glutamine between amino acids 276 and 277 (p.Glu276\_Val277insGln) in the fourth transmembrane  $\alpha$ -helix of peripherin-2 (Figure 8). In 4 of the 5 families where several family members were available, the mutation was found to co-segregate with the disease. Only individual IV:2 of Family PHRC197 harbored the mutation and was presumed to be unaffected, but he was never examined. No common haplotype for 5 microsatellite markers (D6S1575, D6S1549, D6S1552, D6S282, and D6S1650) surrounding PRPH2 was found (data not shown) and the families were not originating from the same area, suggesting that c.829-4C>G could be a mutation hot spot.

#### CLINICAL CHARACTERIZATION OF PATIENTS WITH

**PRPH2 MUTATIONS:** From 27 to 67 patients were available for clinical analysis, depending on the type of examination. On average, the age at presentation was 45.2  $\pm$  17.5 years (n = 44, range 13-78). The initial symptom was night blindness with an apparent age of onset at 30.8  $\pm$  13.8 years (n = 29, range 10-57). Almost half the patients (31/67, 46%) were emmetropic (spherical equivalent 1 to  $\leq$  1), 36% were myopic (SE < -1), and 18% were hypermetropic (SE > 1), showing a skew toward moderate myopia (Figure 5, Top row, left).

We found that cataract, typically present in adult patients with retinitis pigmentosa, was encountered mostly in

patients older than 40 (Figure 5, Top row, right). Visual acuity (VA) (decimal fraction) was variable with age (Figure 5, Middle row, left), 29 of 81 eyes (35.8%) having a normal visual acuity (VA  $\geq$  1) in patients aged 32.3  $\pm$  15.2 years (range 13–61), 34 of 81 eyes (42.0%) having a moderately decreased VA (0.9–0.5) in patients aged 47.9  $\pm$  15.4 years (range 29–78), and 18 of 81 eyes (22.2%) having a severely decreased VA ( $<$ 0.4) in patients aged 61.2  $\pm$  6.4 years (range 43–72). The decrease in VA was significantly correlated with age ( $r = -0.64$ ;  $P < 0.001$ ). The visual field also decreased progressively with age (Figure 5, Middle row, right). We found that 32 of 62 patients (51.6%) kept more than 50% of their visual field, being aged 37.7  $\pm$  13.9 years (range 16–59), while 30 of 62 (48.4%) had lost more than 50%, being aged 54.8  $\pm$  17.6 years (range 16–78). The decrease in visual field was significantly correlated with age ( $r = -0.56$ ;  $P < .001$ ). The rod ERG (dim blue) was recordable (b wave  $>$ 10 mV) in 26 of 60 eyes (43.3%) from patients aged 34.2  $\pm$  16.8 years (range 16–61) and was undetectable in 34 of 60 eyes (56.7%) from patients aged 54.2  $\pm$  11.5 years (range 35–78) (Figure 5, Bottom row, left). The cone ERG (30 Hz flicker) was recordable (b wave amplitude  $>$ 5 mV) in 49 of 54 eyes (90.7%) from patients aged 43.9  $\pm$  18.5 years (range 16–78) and was undetectable in 5 of 54 eyes (10.3%) from patients aged 52.4  $\pm$  6.8 years (range 45–58) (Figure 5, Bottom row, right). Both the rod and the cone ERG decrease was correlated with age,  $r = 0.62$  and  $0.44$ ;  $P < .001$  for rod and cone function, respectively. Fundus examination revealed the presence of pigment deposits in 73% of the patients with a mean age of 45  $\pm$  18 years. Fundus autofluorescence imaging revealed abnormalities in 62.9% (age 47  $\pm$  18 years), including macular autofluorescence ring and atrophic spots in periphery (Table 2). On OCT examination, the majority of patients retained their ellipsoid zone at the fovea (70.4%), whereas a minority had a cystoid macular edema (14.3%). We noticed that some patients had macular involvement with either normal, moderately reduced (Figure 6, Row 1, outer left), or severely decreased (Figure 6, Row 1, inner left) visual acuity. Some patients had a mild RP with a few spots of atrophy in the retinal periphery and macular sparing (Figure 6, Row 1, inner right). In other cases, typical pigment deposits and wide-spread atrophy in the midperipheral retina was present (Figure 6, Row 1, outer right). Some patients showed a pericentral localization of the retinal lesions even if other members of the family had a widespread form (Figure 6, Row 2, outer left). This was particularly evident in Family PHRC281 carrying the p.Pro216Ser (Figure 6, Row 2, inner left to outer right), which a family member (III:2) had a pericentral localization of the retinal lesions sharply delimited from the unaffected peripheral retina while her sister (III:1) had a typical widespread retinitis pigmentosa. In a few circumstances, the presence of yellow deposits was noticed, as in Family PHRC305 carrying the p.Pro216Ser, in which the mother had typical retinitis pigmentosa (Figure 6, Row 3, outer left) and the son a vitelliform foveal deposit but no signs of retinitis pigmentosa (Figure 6, Row 3, inner left).

More clinical details were obtained for the 2 novel recurrent mutations c.761T>A (p.Leu254Gln) and c.829-4C>G (p.Glu276\_Val277insGln), found in 4 and 5 families, respectively. In Family PHRC161 with p.Leu254Gln, the visual acuity of the 2 brothers homozygous for the mutation was severely decreased, with 0.1 at age 63 for Patient II:3 and hand motion on left eye and light perception on right eye at age 71 for Patient II:2. Yet, Patient II:3 still had 0.9 VA on the left eye at age 53, indicating that homozygosity for the mutation did not lead to early-onset severe disease. In general, clinical examination showed a progressive worsening of the visual function with age, with the youngest patients being pauci-symptomatic (Figure 6, Row 3, inner right) until the legal blindness stage in elder patients (Figure 6, Row 3, outer right to Row 4, inner left). In Family PHRC162 with p.Leu254Gln, variability in ERG responses was noticed. Patient II:9, who carried the mutation, still had a recordable scotopic rod ERG response and was asymptomatic, while other mutation carriers of the family had undetectable scotopic ERG rod responses (Figure 7). In the 5 families with c.829-4C>G (p.Glu276\_Val277insGln), the disease was very moderate, the fundus observation being normal (Figure 6, Row 4, inner right) or with moderate lesions (Figure 6, Row 4, outer right) and the ERG responses being recordable, suggesting

that the insertion of an additional amino acid had a moderate pathogenic effect.

## DISCUSSION

Autosomal dominant retinitis pigmentosa is genetically heterogeneous, with 24 known causative genes so far ([www.sph.uth.tmc.edu/retnet](http://www.sph.uth.tmc.edu/retnet)). The present study assessed the prevalence of PRPH2, one of the major genes mutated in adRP, in a large French cohort of 310 families. We established the prevalence of PRPH2 as 10.3% in our cohort, making this gene, after RHO (16.5% in French population<sup>27</sup>), the gene second most frequently found mutated in French adRP patients. Therefore, both genes account for more than a quarter (26.8%) of adRP cases in France. Prevalence studies conducted in the French population revealed that PRPF31 (MIM #606419), with 6.7%,<sup>36</sup> and RP1 (MIM #603937), with 5.3%,<sup>37</sup> are, respectively, the third and fourth most causative genes. Altogether, these 4 genes represent 38.8% of French adRP patients.

Based on the literature, the prevalence of PRPH2 mutations ranges from 0% to 8% of cases of adRP in cohorts of different origins. Mutations in the PRPH2 gene appear to be rare in Southern European adRP patients: 0% (0/48) in Italian<sup>30</sup> and 1% (2/148) in Spanish<sup>38</sup> patients with adRP. In comparison, the proportion of adRP attributable to PRPH2 mutations is higher in populations with Northern European or Asian origins: 3.5% of the Northern American population with altogether dominant and recessive RP (8/227),<sup>21</sup> 5% of Japanese adRP cases (5/96),<sup>9</sup> 8% of American (17/206)<sup>29</sup> and Swedish (3/38)<sup>28</sup> adRP patients. With a prevalence of 10.3% in our cohort, it is higher in France than usually reported, possibly because of underdiagnosed family members with mild disease that we describe in this study, leading to erroneously classifying them as simplex cases. We indeed found that some cases presented as pericentral forms of RP, and other cases are asymptomatic or pauci-symptomatic. In general, we found that the RP associated with PRPH2 mutations is not severe, with many patients retaining useful visual acuity and visual field at middle age. There is no specific refractive error, which distinguishes this RP from the X-linked RP in which myopia is consistently found.<sup>39</sup>

This study reports 15 different mutations in PRPH2 found in 32 families from a cohort of 310 families with adRP; of these, 6 are novel and 9 were previously reported (Table 1). The referenced mutations represent 60% of the mutations identified in this report. Nevertheless, with 40% of novel mutations, it is still worthwhile to screen the whole PRPH2 gene for novel changes.

Among the novel mutations, the deletion c.205delG leads to a premature stop, shortening the protein to 98 residues instead of 346 amino acids (p.Val69Cysfs\*30), and the truncation affects the second transmembrane  $\alpha$ -helix of peripherin-2 (Figure 8) or, more likely, is a functional null allele. To date, 42 truncating mutations including nonsense substitutions and frameshift mutations are listed at the Human Genome Mutation Database (HGMD). Although no DNA samples from additional affected family members were available for segregation analysis, it is likely that the truncating change presented in this study is a pathogenic mutation and causes the RP phenotype in Family PHRC126.

The 4 novel missense changes identified in this study affect evolutionary conserved amino acids (Figure 3) and are located in the large intradiscal loop domain (D2) of peripherin-2 (Figure 8), which contains most disease-causing missense mutations.<sup>40</sup> To date, 124 PRPH2 mutations are listed at the HGMD and approximately 65% of them are located in the D2 loop of the protein, emphasizing the importance of this domain. This D2 loop plays a crucial role in the dimerization of homo- or heterotetramers with ROM1 (retinal outer segment membrane protein 1), the homolog of peripherin-2, to form essential interactions important for disc formation and stabilization.<sup>4-8</sup> The p.Leu254Gln substitution appears to be recurrent in the French population, since it was found in 4 unrelated families with the same geographic origin. All the

affected patients harboring the mutation share the same haplotype for 5 surrounding microsatellite markers (maximum cumulated LOD score of 4.484 for D6S1575), suggesting a founder effect. Two affected brothers (Figure 2, Left, II:2 and II:3 in Family PHRC161) were ho-mozygous for the mutation and were expected to display a more severe phenotype, although this did not seem obvious from clinical records. It is of note that mice with a heterozygous defect in PRPH2 present a loss of photoreceptor outer segment organization while homo-zygous mice have no outer segments.<sup>41,42</sup> Contrary to the null mutation present in mice, the p.Leu254Gln mutation probably acts through a dominant-negative effect by interfering with the dimerization process. The wild-type and mutant (L254Q) peripherin-2 expressed in yeast (Figure 4) migrate as monomers and dimers, but the mutant peripherin-2 shows a pronounced tendency rela-tive to WT to form larger aggregates. This might suggest an abnormal folding for the L254Q mutant. The increased aggregation may disturb homo- and heterotetramers with ROM1 interactions, leading to a loss of some peripherin-2 function.

All novel mutations identified in this study either were located in the D2 loop or truncated the protein before the D2 loop. Nevertheless, 1 mutation (c.829-4C>G), which was predicted to lead to the in-frame insertion of 1 glutamine (p.Glu276\_Val277insGln), was located in the fourth transmembrane  $\alpha$ -helix of peripherin-2 (Figure 8). Three other mutations, within this last trans-membrane  $\alpha$ -helix, are mentioned in the literature; the mutation p.Gly266Asp was found in an adRP patient,<sup>43</sup> the mutation p.Val268Ile was found in a patient with adult vitelliform macular dystrophy,<sup>13</sup> and the in-frame deletion p.Leu271del was identified in a simplex RP pa-tient.<sup>44</sup> The Glu276 residue is conserved in all known peripherin-2 orthologs and is substituted with a glutamine in all known ROM1 orthologs.<sup>45</sup> The significance of this highly conserved glutamic acid at position 276 was inves-tigated for peripherin-2 structure and function.<sup>46</sup> The au-thors created a p.Glu276Gln isosteric substitution, very similar to the p.Glu276\_Val277insGln predicted muta-tion found in our study, and they demonstrated that this conserved residue is critical for outer segment discs morphogenesis. The major physicochemical consequence of the p.Glu276Gln substitution is a loss of ionization potential. They hypothesized that Glu276 may function as a pH sensor to regulate protein activity. Other studies suggest that Glu276 may be important for intramolecular interactions between transmembrane domains.<sup>47,48</sup>

In conclusion, we have established that the prevalence of PRPH2 is 10.3% in a French cohort of 310 adRP individ-uals, which is higher than previously reported. We also established that PRPH2 cause highly variable phenotypes and moderate forms of adRP, including mild cases that could be underdiagnosed. Moreover, mutation analysis in a large cohort is important for the design of future clinical trials.

Nucleotide Change	Exon	Protein Change	Region	PolyPhen2	SIFT	a-GVGD <sup>a</sup>	EVS	Reference
c.136C>T	1	p.Arg46*	D1	N.A.	N.A.	N.A.	0/13 006	Meins et al <sup>49</sup>
c.205delG	1	p.Val69Cysfs*30	2 <sup>nd</sup> TMD	N.A.	N.A.	N.A.	0/13 006	Present study
c.377T>C	1	p.Leu126Pro	D2	Prob.	APF	C65	0/13 006	Renner et al <sup>50</sup>
c.494G>A	1	p.Cys165Tyr	D2	Prob.	APF	C65	0/13 006	Souied et al <sup>51</sup>
c.535T>C	1	p.Trp179Arg	D2	Prob.	APF	C65	0/13 006	Bareil et al <sup>52</sup>
c.582T>A	2	p.Asp194Glu	D2	Pos.	TOL	C35	0/13 006	Present study
c.594C>G	2	p.Ser198Arg	D2	Prob.	APF	C65	0/13 006	Sullivan et al <sup>26</sup>
c.623G>A	2	p.Gly208Asp	D2	Pos.	APF	C65	1/13 006	Kohl et al <sup>35</sup>
c.631T>C	2	p.Phe211Leu	D2	Prob.	APF	C15	0/13 006	Ekstrom et al <sup>53</sup>
c.646C>T	2	p.Pro216Ser	D2	Pos.	TOL	C65	0/13 006	Fishman et al <sup>54</sup>
c.664T>A	2	p.Cys222Ser	D2	Prob.	APF	C65	0/13 006	Downs et al <sup>55</sup>
c.738G>C	2	p.Trp246Cys	D2	Prob.	APF	C65	0/13 006	Present study
c.758C>A	2	p.Ala253Glu	D2	Prob.	TOL	C65	0/13 006	Present study
c.761T>A	2	p.Leu254Gln	D2	Prob.	APF	C65	0/13 006	Present study
c.829-4C>G	Int. 2-3	Splice site defect (p.Glu276_Val277insGln)	4 <sup>th</sup> TMD	N.A.	N.A.	N.A.	0/13 006	Present study

D1 ¼ D1 loop; D2 ¼ D2 loop; TMD ¼ transmembrane helical domain; N.A. ¼ not applicable; Int. ¼ intron; EVS ¼ exome variant server; Pos. ¼ possibly damaging; Prob. ¼ probably damaging; APF ¼ affect protein function; TOL ¼ tolerated.

<sup>a</sup>a-GVGD scores: amino acid substitutions on a 7-scale scoring system, from C0 (neutral) to C65 (the most likely pathogenic); C35 is considered intermediate.

TABLE 1. Summary of *PRPH2* Gene Mutations Identified in This Study in Patients With Autosomal Dominant Retinitis Pigmentosa

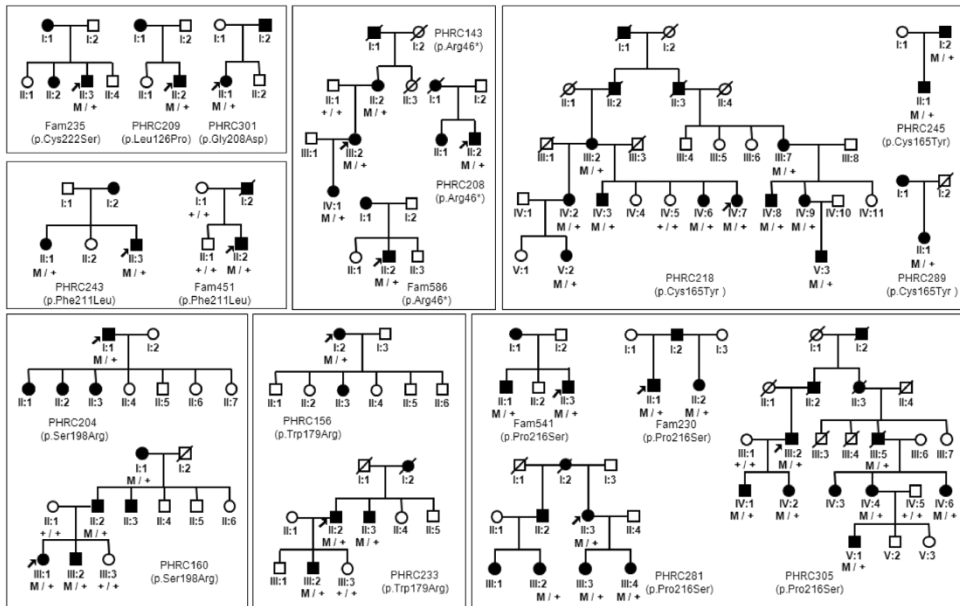


FIGURE 1. Pedigrees of French families with autosomal dominant retinitis pigmentosa and with recurrent mutations in PRPH2 gene identified in this study. Filled symbols indicate affected family members; squares: male subjects; circles: female subjects; arrows: in-dex patients. (Top left) Family pedigrees of patients showing different recurrent PRPH2 mutations. (Top middle) Families with c.136C>T (p.Arg46\*) mutation. (Top right) Families with c.494G>A (p.Cys165Tyr) mutation. (Middle left) Families with c.631T>C (p.Phe211Leu) mutation. (Bottom left) Families with c.594C>G (p.Ser198Arg) mutation. (Bottom middle) Families with c.535T>C (p.Trp179Arg) mutation. (Bottom right) Families with c.646C>T (p.Pro216Ser) mutation.

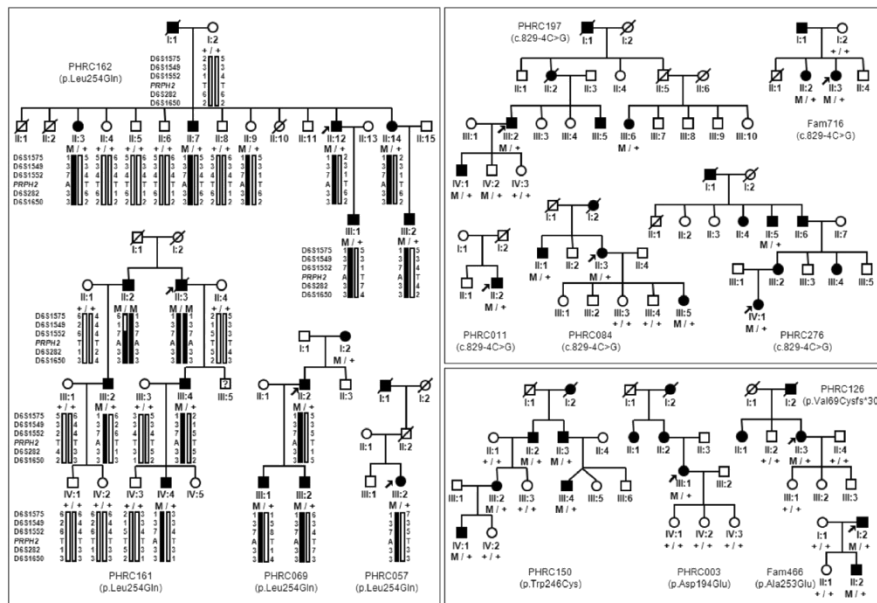


FIGURE 2. Pedigrees of French families with autosomal dominant retinitis pigmentosa and with novel mutations in PRPH2 gene identified in this study. (Left) Haplotypes at the PRPH2 locus of 4 families showing the c.761T>A (p.Leu254Gln) mutation and surrounding microsatellite markers. The common haplotype is shown in black. (Top right) Five families with c.829-4C>G splice site mutation. (Bottom right) Family pedigrees of patients showing different novel PRPH2 mutations.

	Asp194		Trp246	Ala253	Leu254
Human	▼	SKEVKDRIKSN ...	▼	▼	EELNLWVRGCRAALLSYYS
Chimpanzee		SKEVKDRIKSN ...			EELNLWVRGCRAALLSYYS
Gorilla		SKEVKDRIKSN ...			EELNLWVRGCRAALLSYYS
Dog		SKEVKDRIKSN ...			EELNLWVRGCRAALLSYYS
Cat		SKEVKDRIKSN ...			EELNLWVRGCRAALLSYYG
Cow		SKEVKDRIKSN ...			EELNLWVRGCRAALLSYYS
Horse		SKEVKDRIKSN ...			EELNLWVRGCRAALLGYYS
Elephant		SKEVKDRVKSN ...			EELNLWVRGCRDALLSYYS
Rabbit		SKEVKDRIKSN ...			EELNLWVRGCRDALLSYYS
Mouse		SKEVKDRIKSN ...			EELNLWVRGCRAALLNYYS
Chicken		SKEVKDRIKSN ...			EELNLWVRGCRAALLHYYS
Zebra finch		SKEVKDRIKSN ...			EELNLWVRGCRAALLNYYS
Dolphin		SKEVKDRIKSN ...			EELNLWVRGCRAALLSYYS
Platypus		SKEVKDRIKSN ...			EELNLWVRGCRAALLFYYS
Tetraodon		AKEVKDRIGSN ...			EELNVWVRGCRAALLSYYG
Tilapia		SKEVDRIGSN ...			EDLNVWVRGCRAALLSYYG
Xenopus		SKEVKDRIKSN ...			EELNLWVRGCRAALLTYYT

FIGURE 3. Conservation of amino acids affected by novel PRPH2 missense mutations identified in this study in patients with autosomal dominant retinitis pigmentosa. Multiple amino acid sequence alignment of peripherin-2 for a region surrounding the novel p.Asp194Glu, p.Trp246Cys, p.Ala253Glu, and p.Leu254Gln missense mutations. The site of the mutation is indicated by an arrowhead.

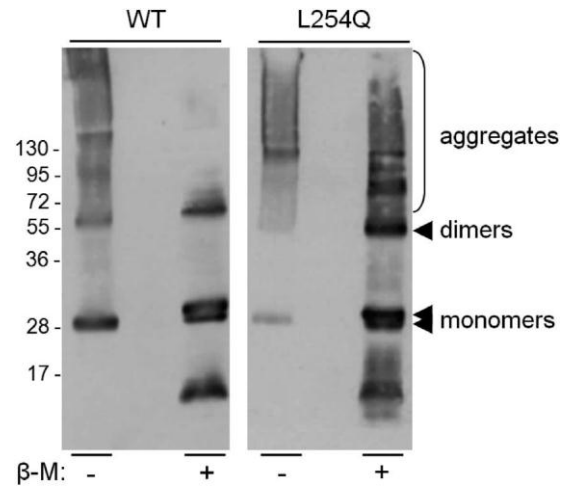


FIGURE 4. Western blot analysis of wild-type and p.Leu254Gln mutant peripherin-2 protein produced in yeast. Western blots of the wild-type (WT) and the mutated p.Leu254Gln (L254Q) peripherin-2 from *P. pastoris* purified with Ni-NTA superflow agarose in the presence (D) or in the absence (L) of the reducing agent b-mercaptoethanol (b-M) in the sample buffer. The blot was probed with a monoclonal anti-c-myc antibody.

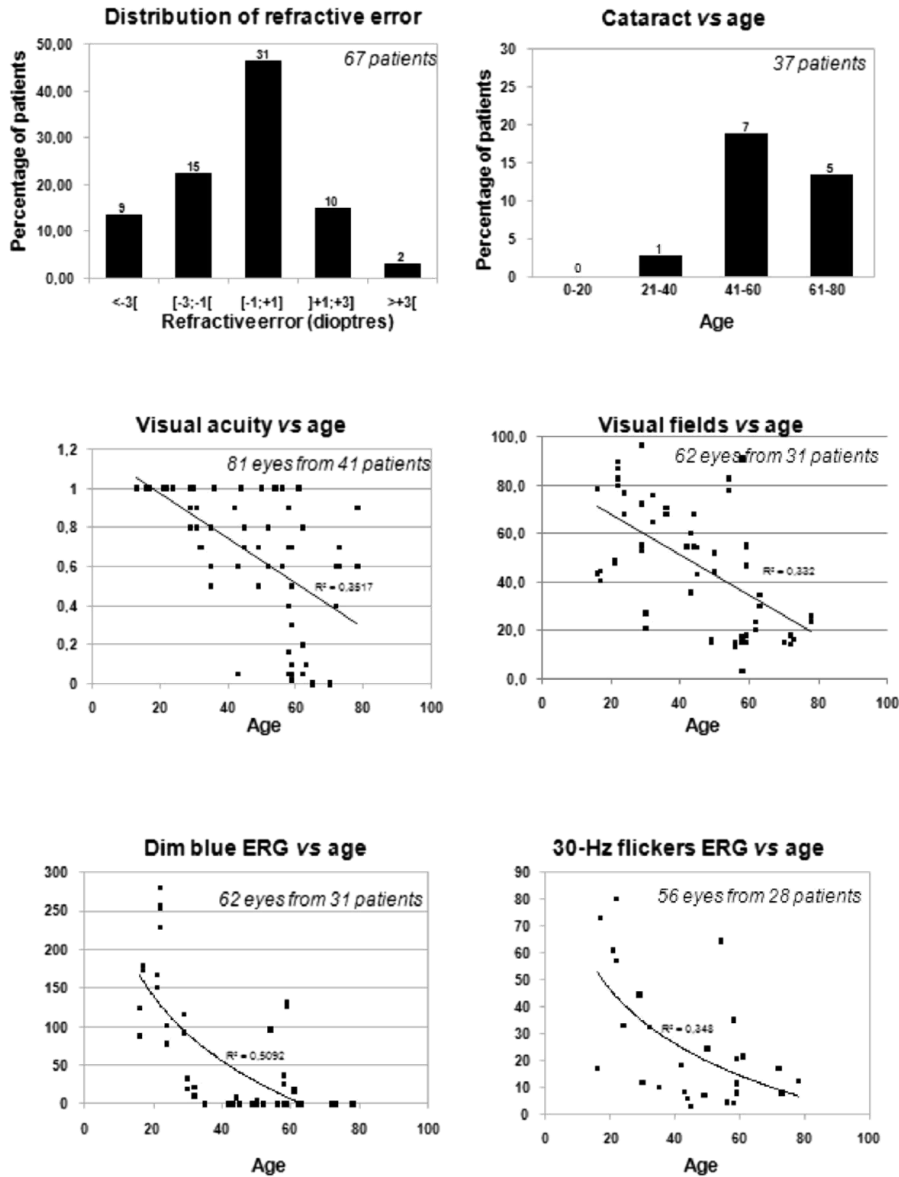


FIGURE 5. Clinical data of the patients with autosomal dominant retinitis pigmentosa and with PRPH2 gene mutations. (Top row, left) Refractive errors were classified in 5 groups as either severe myopia (<L3[), moderate myopia ([L3;L1[), emmetropia ([L1;D1]), moderate hyperopia ([D1;D3]), or severe hyperopia (>D3[) and the percentage (y-axis) and the absolute number (above each bar) of patients are given for each group. (Top row, right) Apparent onset of cataract was classified in 4 groups depending on age and the percentage (y-axis) and the absolute number (above each bar) of patients are given for each group. Visual acuity in decimal values (Middle row, left), percentage of remaining Goldmann visual field (Middle row, right), b-wave amplitude of the dim blue electroretinogram (ERG) testing rods (Bottom row, left), and peak-to-peak amplitude of the 30 Hz flicker ERG testing cone function (Bottom row, right) were plotted against age.

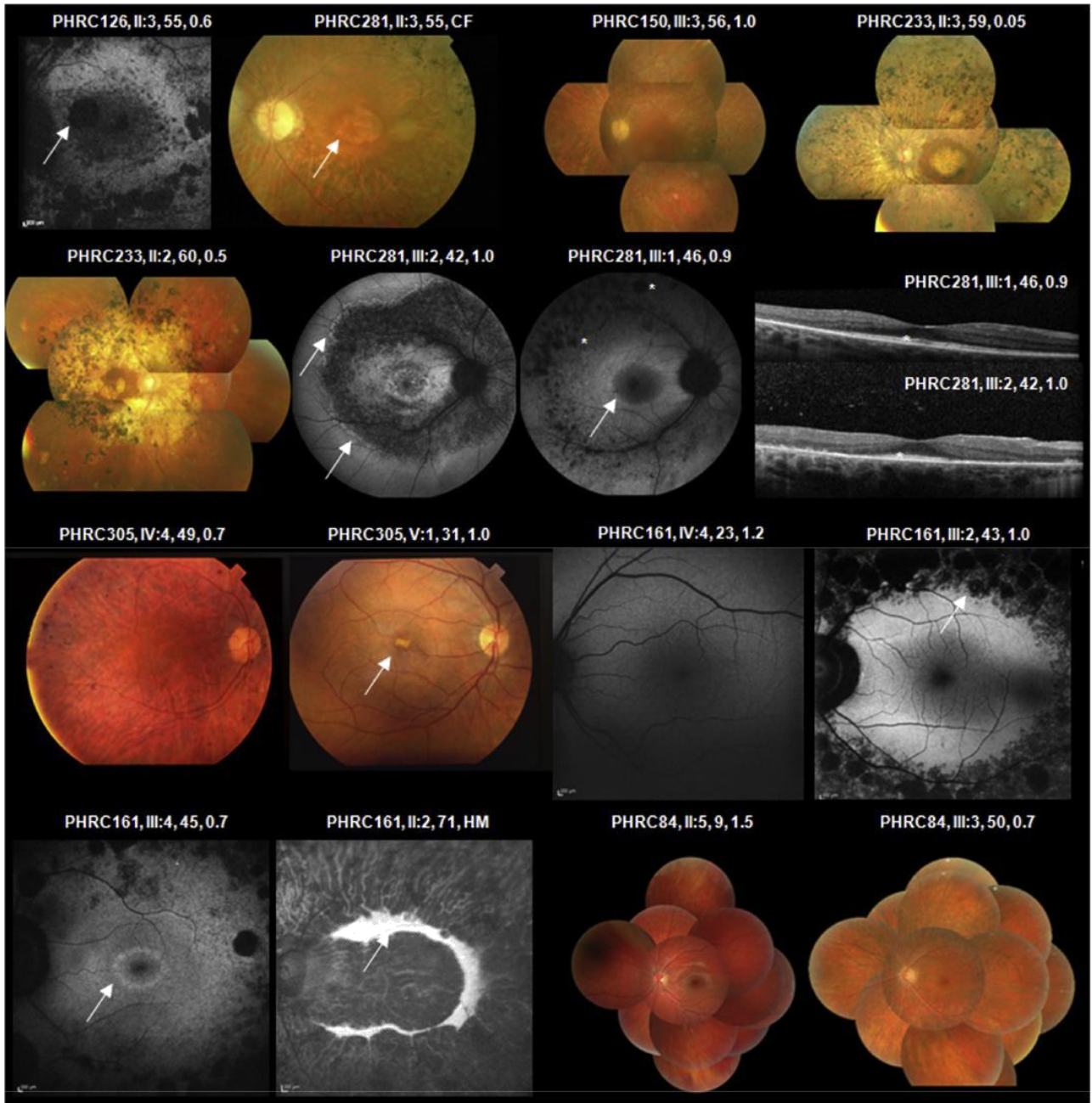


FIGURE 6. Fundus imaging of patients with autosomal dominant retinitis pigmentosa and with PRPH2 gene mutations. On top of each picture (fundus photographs, fundus autofluorescence [FAF] photographs, and spectral-domain optical coherence tomography [OCT] scans), the family number (PHRC), patient number in the family, age, and visual acuity in decimal values are indicated. (Row 1, outer left) Left eye FAF, macular alteration, parafoveal loss of autofluorescence (arrow) with moderate decrease in visual acuity. (Row 1, inner left) Left eye color fundus photograph, pale optic disc, narrow blood vessels, pigmentary changes in the periphery, and RPE changes in the macular region (arrow) correlated with severe loss of visual acuity at counting fingers (CF). (Row 1, inner right) Left eye color fundus photographs; there are a few small spots of atrophy in the retinal periphery and the macula appears normal. (Row 1, outer right, and Row 2, outer left) Color fundus photographs from 2 affected brothers, with, for the left eye of Patient II:3, round foveal atrophy and pigment deposits covering a large proportion of the fundus, while for the right eye of the Patient II:2, most of the retinal atrophy and pigment deposits are present in the macular area. (Row 2, inner left to outer right) FAF and OCT of right eyes from 2 sisters, with, for Patient III:2, a pericentral form of retinitis pigmentosa with alteration of autofluorescence within the macular area and sharp limit of the lesions (arrows), while the sister, Patient III:1, has a typical widespread retinitis pigmentosa showing small spots of retinal atrophy (stars) and a ring of autofluorescence (white arrow); OCT scans of the macula in both sisters show a conserved inner segment/outer segment line (stars) in the fovea. (Row 3, outer left and inner left) The mother, Patient IV:4, has retinitis pigmentosa with pigment deposits in the retinal periphery while the son, V:1, has a foveal yellow vitelliform deposit (arrow) but

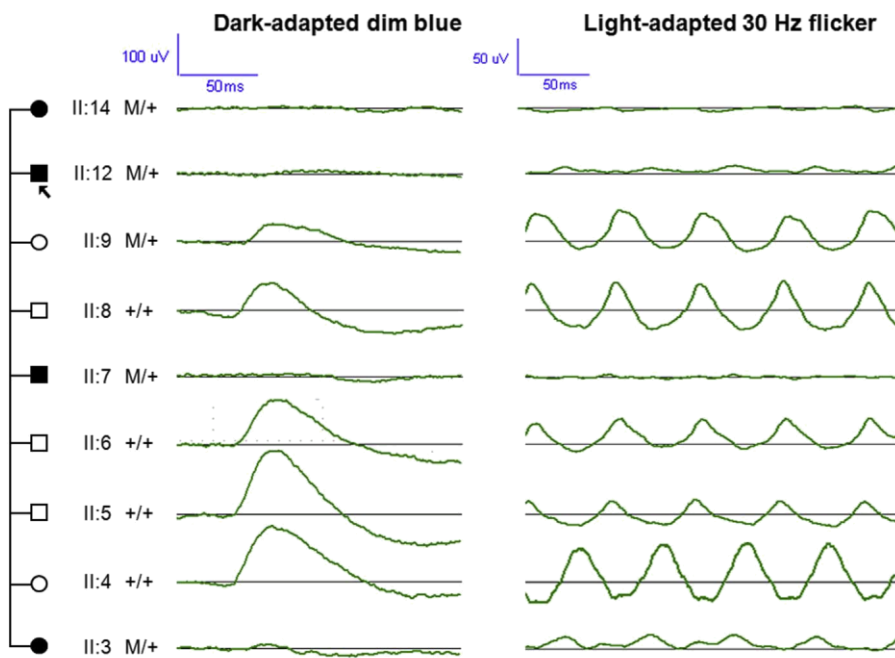


FIGURE 7. Variability of electroretinographic responses in Family PHRC162 with autosomal dominant retinitis pigmentosa and with the PRPH2 gene mutation p.Leu254Gln. Each patient from generation II in PHRC162 was subjected to dark-adapted dim blue stimulation for rod responses and light-adapted 30 Hz flicker for cone responses. Black symbols indicate symptomatic patients, open symbols nonaffected or asymptomatic patients. Genotypes are shown. The 4 affected patients (II:3, II:7, II:12, and II:13) have no rod responses and severely decreased cone responses, while the asymptomatic carrier II:9 still has rod responses, although decreased in comparison to normal responses in II:4, II:5, II:6, and II:8. retinitis no pigmentosa. (Row 3, inner right to Row 4, inner left) FAF imaging in 4 members of the PHRC161 family; the youngest member, IV:4, has no retinal alteration, member III:2 has many round spots of loss of autofluorescence beyond the macula (arrow) but the macula is normal, member III:4 has a similar aspect to III:2 but there is a ring of autofluorescence around the fovea with moderate decrease of visual acuity, and the oldest member, II:2, has a complete loss of autofluorescence except for an open ring of remaining retina around the foveal area (arrow) and visual acuity reduced to hand motion (HM). (Row 4, inner right and outer right) Fundus photographs of the daughter, II:5, show retinal lesion and slightly reduced retinal vessel diameter while fundus photographs of the mother, III:3, revealed changes typical of retinitis pigmentosa, with overall moderate RPE changes and attenuated retinal vessels but no pigment deposits.

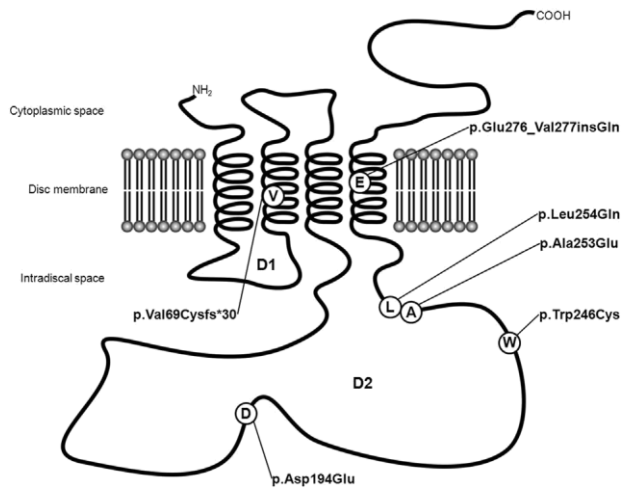


FIGURE 8. Summary of the novel mutations found in this study in peripherin-2 protein and in patients with autosomal dominant retinitis pigmentosa. Schematic representation of the peripherin-2 protein showing the location of the 6 novel mutations presented in this study. The 4 transmembrane  $\alpha$ -helices and the 2 intradiscal loop domains D1 and D2 are schematized.

TABLE 2. Frequency of Clinical Features in Patients With Autosomal Dominant Retinitis Pigmentosa and *PRPH2* Gene Mutation

Description	Mean Age (y)	Number of Patients	Percentage of Positive Cases
Pigment deposits	45 6 18	37	73.0%
Autofluorescence changes	47 6 18	35	62.9%
Cystoid macular edema	43 6 17	28	14.3%
Conserved ellipsoid zone	43 6 17	27	70.4%

## REFERENCES

1. Arikawa K, Molday LL, Molday RS, Williams DS. Localization of peripherin/rds in the disk membranes of cone and rod photoreceptors: relationship to disk membrane morphogenesis and retinal degeneration. *J Cell Biol* 1992;116(3):659–667.
2. Connell G, Bascom R, Molday L, Reid D, McInnes RR, Molday RS. Photoreceptor peripherin is the normal product of the gene responsible for retinal degeneration in the rds mouse. *Proc Natl Acad Sci U S A* 1991;88(3):723–726.
3. Molday RS, Hicks D, Molday L. Peripherin. A rim-specific membrane protein of rod outer segment discs. *Invest Ophthalmol Vis Sci* 1987;28(1):50–61.
4. Boesze-Battaglia K, Lamba OP, Napoli AA Jr, Sinha S, Guo Y. Fusion between retinal rod outer segment membranes and model membranes: a role for photoreceptor peripherin/ rds. *Biochemistry* 1998;37(26):9477–9487.
5. Goldberg AF, Molday RS. Subunit composition of the peripherin/rds-rom-1 disk rim complex from rod photoreceptors: hydrodynamic evidence for a tetrameric quaternary structure. *Biochemistry* 1996;35(19):6144–6149.
6. Loewen CJ, Molday RS. Disulfide-mediated oligomerization of Peripherin/Rds and Rom-1 in photoreceptor disk membranes. Implications for photoreceptor outer segment morphogenesis and degeneration. *J Biol Chem* 2000;275(8): 5370–5378.
7. Molday RS. Photoreceptor membrane proteins, phototransduction, and retinal degenerative diseases. The Friedenwald Lecture. *Invest Ophthalmol Vis Sci* 1998;39(13):2491–2513.
8. Travis GH, Sutcliffe JG, Bok D. The retinal degeneration slow (rds) gene product is a photoreceptor disc membrane-associated glycoprotein. *Neuron* 1991;6(1):61–70.
9. Kajiwara K, Hahn LB, Mukai S, Travis GH, Berson EL, Dryja TP. Mutations in the human retinal degeneration slow gene in autosomal dominant retinitis pigmentosa. *Nature* 1991;354(6353):480–483.
10. Nakazawa M, Kikawa E, Chida Y, Tamai M. Asn244His mutation of the peripherin/RDS gene causing autosomal dominant cone-rod degeneration. *Hum Mol Genet* 1994;3(7): 1195–1196.
11. Nakazawa M, Kikawa E, Chida Y, Wada Y, Shiono T, Tamai M. Autosomal dominant cone-rod dystrophy associated with mutations in codon 244 (Asn244His) and codon 184 (Tyr184Ser) of the peripherin/RDS gene. *Arch Ophthalmol* 1996;114(1):72–78.
12. Kajiwara K, Sandberg MA, Berson EL, Dryja TP. A null mutation in the human peripherin/RDS gene in a family with autosomal dominant retinitis punctata albescens. *Nat Genet* 1993;3(3):208–212.
13. Felbor U, Schilling H, Weber BH. Adult vitelliform macular dystrophy is frequently associated with mutations in the peripherin/RDS gene. *Hum Mutat* 1997;10(4):301–309.
14. Fishman GA, Stone EM, Alexander KR, Gilbert LD, Derlacki DJ, Butler NS. Serine-27-phenylalanine mutation within the peripherin/RDS gene in a family with cone dystrophy. *Ophthalmology* 1997;104(2):299–306.
15. Keen TJ, Inglehearn CF, Kim R, Bird AC, Bhattacharya S. Retinal pattern dystrophy associated with a 4 bp insertion at codon 140 in the RDS-peripherin gene. *Hum Mol Genet* 1994;3(2):367–368.
16. Kim RY, Dollfus H, Keen TJ, et al. Autosomal dominant pattern dystrophy of the retina associated with a 4-base pair insertion at codon 140 in the peripherin/RDS gene. *Arch Ophthalmol* 1995;113(4):451–455.
17. Hoyng CB, Heutink P, Testers L, Pinckers A, Deutman AF, Oostra BA. Autosomal dominant central areolar choroidal dystrophy caused by a mutation in codon 142 in the peripherin/RDS gene. *Am J Ophthalmol* 1996;121(6):623–629.
18. Piguet B, He´on E, Munier FL, et al. Full characterization of the maculopathy associated with an Arg-172-Trp mutation in the RDS/peripherin gene. *Ophthalmic Genet* 1996;17(4): 175–186.
19. Wells J, Wroblewski J, Keen J, et al. Mutations in the human retinal degeneration slow (RDS) gene can cause either retinitis pigmentosa or macular dystrophy. *Nat Genet* 1993; 3(3):213–218.
20. Yanagihashi S, Nakazawa M, Kurotaki J, Sato M, Miyagawa Y, Ohguro H. Autosomal dominant central areolar choroidal dystrophy and a novel Arg195Leu mutation in the peripherin/ RDS gene. *Arch Ophthalmol* 2003;121(10):1458–1461.
21. Dryja TP, Hahn LB, Kajiwara K, Berson EL. Dominant and digenic mutations in the peripherin/RDS and ROM1 genes in retinitis pigmentosa. *Invest Ophthalmol Vis Sci* 1997; 38(10):1972–1982.

23. Kajiwara K, Berson EL, Dryja TP. Digenic retinitis pigmentosa due to mutations at the unlinked peripherin/RDS and ROM1 loci. *Science* 1994;264(5165):1604–1608.
24. Hartong DT, Berson EL, Dryja TP. Retinitis pigmentosa. *Lancet* 2006;368(9549):1795–1809.
25. Haim M. Epidemiology of retinitis pigmentosa in Denmark. *Acta Ophthalmol Scand Suppl* 2002;233:1–34.
26. Dryja TP, McGee TL, Reichel E, et al. A point mutation of the rhodopsin gene in one form of retinitis pigmentosa. *Nature* 1990;343(6256):364–366.
27. Sullivan LS, Bowne SJ, Birch DG, et al. Prevalence of disease-causing mutations in families with autosomal dominant retinitis pigmentosa: a screen of known genes in 200 families. *Invest Ophthalmol Vis Sci* 2006;47(7): 3052–3064.
28. Audo I, Manes G, Mohand-Said S, et al. Spectrum of rhodopsin mutations in French autosomal dominant rod-cone dystrophy patients. *Invest Ophthalmol Vis Sci* 2010; 51(7):3687–3700.
29. Ekstrom U, Ponjavic V, Andreasson S, Ehinger B, Nilsson-Ehle P, Abrahamson M. Detection of alterations in all three exons of the peripherin/RDS gene in Swedish patients with retinitis pigmentosa using an efficient DGGE system. *Mol Pathol* 1998;51(5):287–291.
30. Sohocki MM, Daiger SP, Bowne SJ, et al. Prevalence of mutations causing retinitis pigmentosa and other inherited retinopathies. *Hum Mutat* 2001;17(1):42–51.
31. Ziviello C, Simonelli F, Testa F, et al. Molecular genetics of autosomal dominant retinitis pigmentosa (ADRP): a comprehensive study of 43 Italian families. *J Med Genet* 2005;42(7): e47.
32. Marmor MF, Fulton AB, Holder GE, et al. ISCEV Standard for full-field clinical electroretinography (2008 update). *Doc Ophthalmol* 2009;118(1):69–77.
33. Miller SA, Dykes DD, Polesky HF. A simple salting out procedure for extracting DNA from human nucleated cells. *Nucleic Acids Res* 1988;16(3):1215.
34. Vos WL, Vaughan S, Lall PY, McCaffrey JG, Wysocka-Kapcinska M, Findlay JBC. Expression and structural characterization of peripherin/RDS, a membrane protein implicated in photoreceptor outer segment morphology. *Eur Biophys J* 2010;39(4):679–688.
35. Jacobson SG, Cideciyan AV, Kemp CM, Sheffield VC, Stone EM. Photoreceptor function in heterozygotes with insertion or deletion mutations in the RDS gene. *Invest Ophthalmol Vis Sci* 1996;37(8):1662–1674.
36. Kohl S, Christ-Adler M, Apfelstedt-Sylla E, et al. RDS/peripherin gene mutations are frequent causes of central retinal dystrophies. *J Med Genet* 1997;34(8):620–626.
37. Audo I, Bujakowska K, Mohand-Said S, et al. Prevalence and novelty of PRPF31 mutations in French autosomal dominant rod-cone dystrophy patients and a review of published reports. *BMC Med Genet* 2010;11:145.
38. Audo I, Mohand-Said S, Dhaenens C-M, et al. RP1 and autosomal dominant rod-cone dystrophy: novel mutations, a review of published variants, and genotype-phenotype correlation. *Hum Mutat* 2012;33(1):73–80.
39. Milla E, Maseras M, Martınez-Gimeno M, et al. [Genetic and molecular characterization of 148 patients with autosomal dominant retinitis pigmentosa (ADRP)]. *Arch Soc Esp Ophthalmol* 2002;77(9):481–484.
40. Kaplan J, Pelet A, Martin C, et al. Phenotype-genotype correlations in X linked retinitis pigmentosa. *J Med Genet* 1992; 29(9):615–623.
41. Boon CJF, den Hollander AI, Hoyng CB, Cremers FPM, Klevering BJ, Keunen JEE. The spectrum of retinal dystrophies caused by mutations in the peripherin/RDS gene. *Prog Retin Eye Res* 2008;27(2):213–235.
42. Hawkins RK, Jansen HG, Sanyal S. Development and degeneration of retina in rds mutant mice: photoreceptor abnormalities in the heterozygotes. *Exp Eye Res* 1985;41(6):701–720.
43. Sanyal S, Jansen HG. Absence of receptor outer segments in the retina of rds mutant mice. *Neurosci Lett* 1981;21(1):23–26.
44. Kajiwara K, Berson EL, Dryja TP. Screen for mutations in the entire coding sequence of the human RDS/peripherin gene in patients with hereditary retinal degenerations. *Invest Ophthalmol Vis Sci* 1992;33(4):1149–1151.
45. Jin Z-B, Mandai M, Yokota T, et al. Identifying pathogenic genetic background of simplex or multiplex retinitis pigmentosa patients: a large scale mutation screening study. *J Med Genet* 2008;45(7):465–472.

46. Goldberg AFX. Role of peripherin/rds in vertebrate photoreceptor architecture and inherited retinal degenerations. *Int Rev Cytol* 2006;253:131–175.
47. Goldberg AFX, Ritter LM, Khattree N, et al. An intramembrane glutamic acid governs peripherin/rds function for photoreceptor disk morphogenesis. *Invest Ophthalmol Vis Sci* 2007;48(7):2975–2986.
48. Kovalenko OV, Metcalf DG, DeGrado WF, Hemler ME. Structural organization and interactions of transmembrane domains in tetraspanin proteins. *BMC Struct Biol* 2005;5:11.
49. Seigneuret M. Complete predicted three-dimensional structure of the facilitator transmembrane protein and hepatitis C virus receptor CD81: conserved and variable structural domains in the tetraspanin superfamily. *Biophys J* 2006; 90(1):212–227.
50. Meins M, Grünig G, Blankenagel A, et al. Heterozygous ‘‘null allele’’ mutation in the human peripherin/RDS gene. *Hum Mol Genet* 1993;2(12):2181–2182.
51. Renner AB, Fiebig BS, Weber BHF, et al. Phenotypic variability and long-term follow-up of patients with known and novel PRPH2/RDS gene mutations. *Am J Ophthalmol* 2009; 147(3):518–530.
52. Souied EH, Rozet JM, Gerber S, et al. Two novel missense mutations in the peripherin/RDS gene in two unrelated French patients with autosomal dominant retinitis pigmentosa. *Eur J Ophthalmol* 1998;8(2):98–101.
53. Bareil C, Delague V, Arnaud B, Demaille J, Hamel C, Claustres M. W179R: a novel missense mutation in the peripherin/RDS gene in a family with autosomal dominant retinitis pigmentosa. *Hum Mutat* 2000;15(6):583–584.
54. Ekström U, Ponjavic V, Abrahamson M, et al. Phenotypic expression of autosomal dominant retinitis pigmentosa in a Swedish family expressing a Phe-211-Leu variant of peripherin/RDS. *Ophthalmic Genet* 1998;19(1):27–37.
55. Fishman GA, Stone E, Gilbert LD, Vandenburg K, Sheffield VC, Heckenlively JR. Clinical features of a previously undescribed codon 216 (proline to serine) mutation in the peripherin/retinal degeneration slow gene in autosomal dominant retinitis pigmentosa. *Ophthalmology* 1994;101(8): 1409–1421.
56. Downs K, Zacks DN, Caruso R, et al. Molecular testing for hereditary retinal disease as part of clinical care. *Arch Ophthalmol* 2007;125(2):252–258.

